Supporting Information

Rubin *et al.* 10.1073/pnas.0808776106

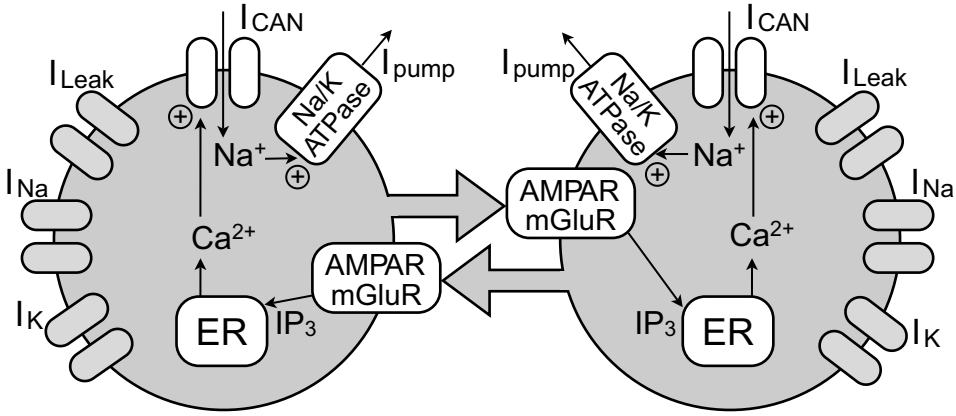

Fig. S1. Schematic diagram of the model. Reciprocally coupled neurons motivated by respiratory neurons of the mammalian preBötC were equipped with Hodgkin-Huxley-style ''fast'' Na^+ and delayed-rectifier K^+ currents (I_{Na}, I_K), and a K^+-dominated leakage current (I_{Leak}). I_{Na}, I_K, and I_{Leak} are shaded gray to indicate that their role is mostly in setting resting potential and generating spikes. As discussed in the text, the bursting dynamics in the model depend on a Ca^{2+}-activated nonspecific cationic current (I_{CAN}), material balance equations that determine the intracellular concentrations of Ca^{2+} and Na^+, and some type of activity-dependent net outward current (Figs. 3 and 4 and Figs. S3 and S4). In the basic model illustrated, the net outward current is mediated by an Na/K ATPase pump (I_{pump}), as analyzed in Figs. 3, S3A, and S4A. Other net outward currents included a voltage-dependent M-like K^+ current (I_M, Fig. 4*A* and Figs. S3*B* and S4*B*), Ca^{2+}-dependent K^+ current ($I_{K\text{-}Ca}$, Fig. 4*B* and Figs. S3*C* and S4*C*), and voltage-dependent inactivation of inward persistent Na^+ current (I_{NaP}, Fig. 4*C* and Figs. S3*D* and S4*D*).

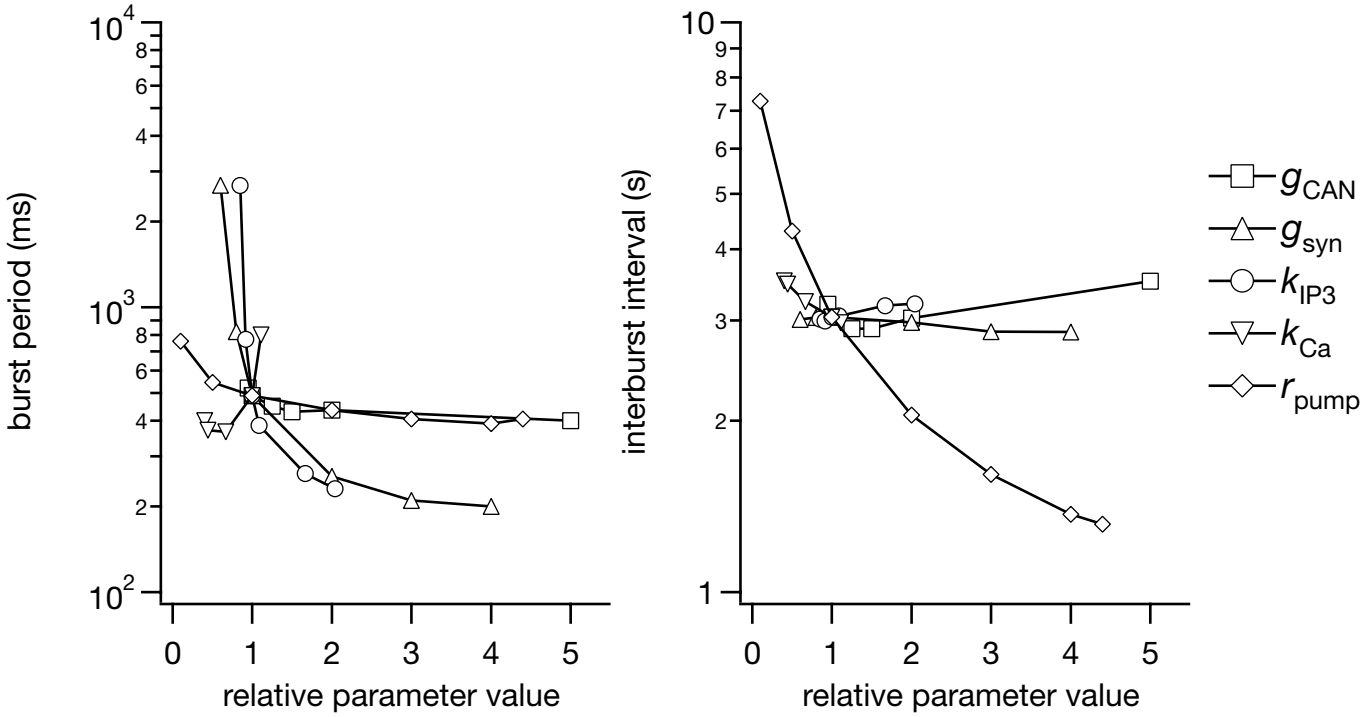

Fig. S2. Robustness parameter study in the self-coupled model with I_{pump}. Burst period (*Left*) and interburst interval (*Right*), plotted over the range of each parameter for which the self-coupled neuron generated rhythmic bursts. Such bursts were defined as trajectories analogous to Fig. 3*D*, with a pair of AH crossings followed by a pair of SNIC crossings in the (Ca^{2+}-Na^{+}) plane in each period. Each parameter value was normalized relative to its default value (see *Derivation of the model*, *SI Appendix*). The parameters varied include: g_{CAN} (squares), g_{syn} (upward triangles), k_{IP3} (circles), k_{ca} (downward triangles), and r_{pump} (diamonds).

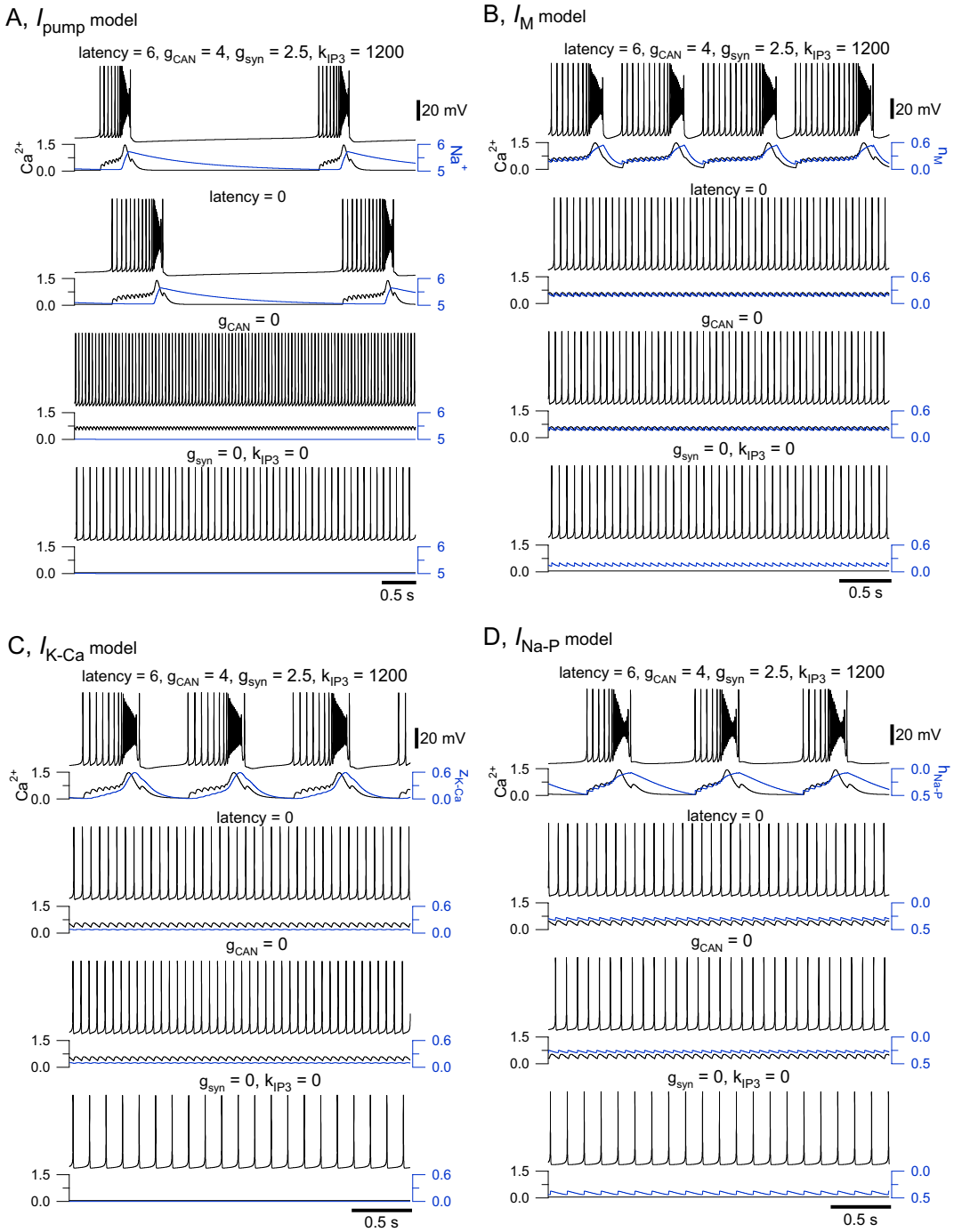

Fig. S3. Simulations of the self-coupled model using different net outward currents, showing that the parameters g_{CAN}, g_{syn}, and k_{IP3} and the currents they influence are critical, regardless of which activity-dependent net outward current is used in the model. (*A–D*) Sets of 4 time courses of model outputs. Each sweep consists of 3 traces: membrane potential (*Upper*, black), Ca^{2+} (*Lower*, black), and the model-specific slow variable (*Lower,* blue, superimposed with Ca^{2+} dynamics). The upper sweep in each panel serves as control and lists default standard parameter values for latency, g_{CAN}, g_{syn}, and k_{IP3}. Subsequent (*Lower*) sweeps in each panel each show results given by varying one or more of the parameters from the control condition. (*A*) I_{pump} model with Na^+ as the slow variable. (*B*) I_M model with n_M as the slow variable. (*C*) $I_{K\text{-}Ca}$ model with $z_{K\text{-}Ca}$ as the slow variable. (*D*) I_{NaP} model with h_{NaP} as the slow variable.

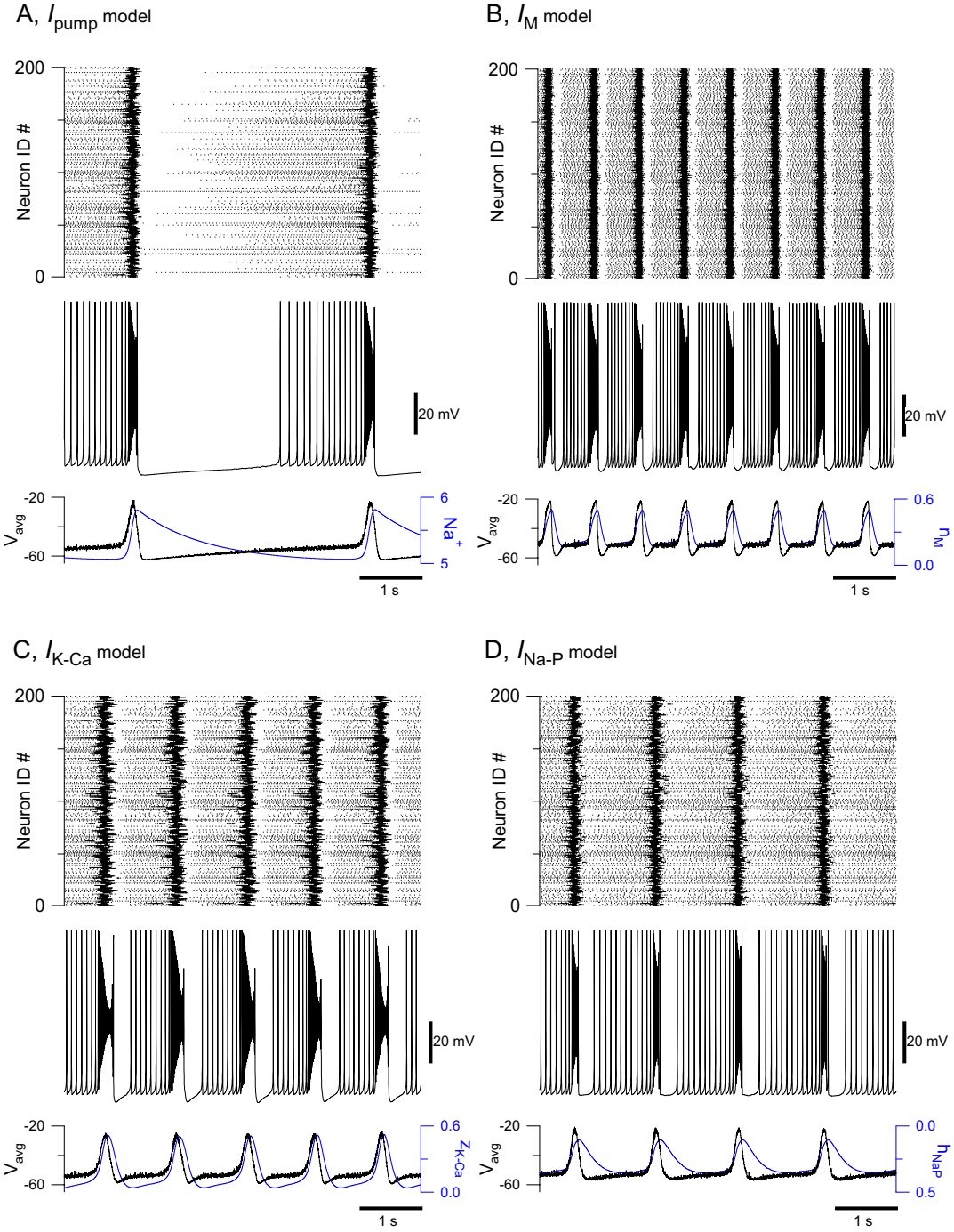

Fig. S4. Rhythmic burst activity in large-scale network models. Each panel consists of a raster diagram (*Top*) showing the spike times of 200 simulated neurons, the voltage trajectory of a representative neuron (*Middle*), the average membrane voltage for all neurons in the network (*Bottom*, black) along with the average slow variable (blue). (*A*–*D*) Network activity with different activity-dependent outward currents including I_{pump}, where average Na^+ concentration is the slow variable (*A*), M-like K^+ current (I_M), where average n_M is the slow variable (*B*), Ca^{2+}-dependent K^+ current ($I_{K\text{-}Ca}$), where average $z_{K\text{-}Ca}$ is the slow variable (*C*), and persistent Na^+ current (I_{NaP}), where average $h_{Na\text{-}P}$ is the slow variable (*D*).

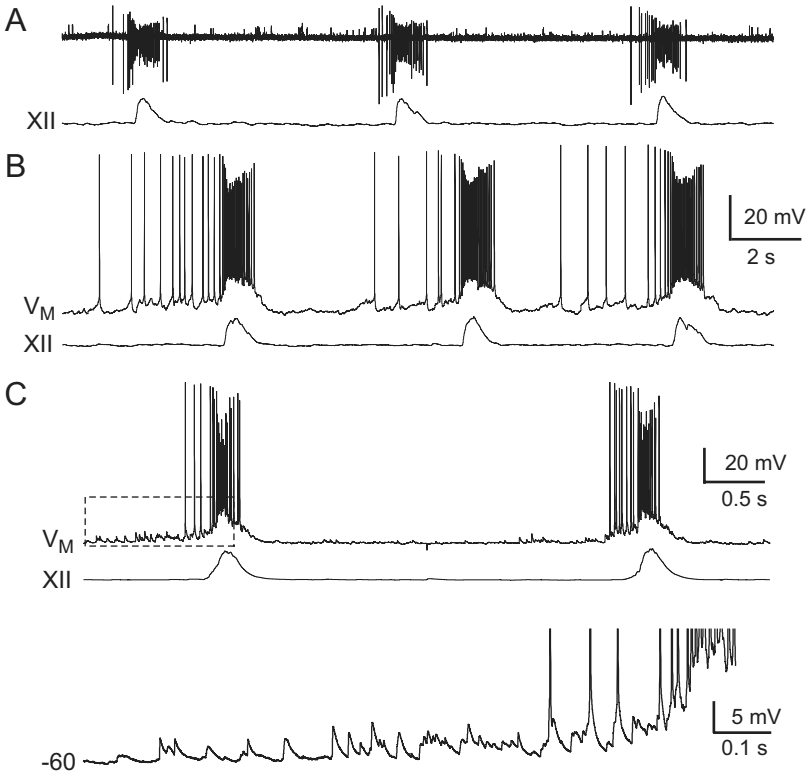

Fig. S5. Respiratory rhythm generation in vitro. (*A*) On-cell patch recording of a preBötC neuron (*Upper*) with inspiratory motor discharge recorded from the hypoglossal (XII) motor nerve root (*Lower*). (*B*) Whole-cell recording conditions in the same cell as A (*Upper*) with XII motor output (*Lower*). Baseline membrane potential was −60 mV. (*C*) Two consecutive cycles in a representative preBötC neuron (top trace) with XII motor output (lower trace). Ramp-like depolarization and EPSPs occur 300-1000 ms before the inspiratory phase; spiking occurs in the final 300 ms before the inspiratory phase. Voltage-dependent spike inactivation, i.e., depolarization block, is visible during the inspiratory bursts. Temporal summation of EPSPs and low-rate (≈5–10 Hz) spiking activity in the preBötC shows evidence for recurrent synaptic excitation during respiratory rhythmogenesis. Broken lines indicate the region of the recording that is expanded in the *Inset*. (*Inset*) Illustrates temporal summation of EPSPs and preinspiratory spiking in greater detail.

Other Supporting Information Files

SI Appendix